In-fiber directional coupler for high-sensitivity curvature measurement

J. R. Guzman-Sepulveda and D. A. May-Arrioja*

Fiber and Integrated Optics Laboratory, UAM Reynosa-Rodhe, Universidad Autónoma de Tamaulipas, Carr. Reynosa-San Fernando S/N, Reynosa, Tamaulipas 88779, México

**darrioja@uat.edu.mx*

Abstract: A curvature fiber optic sensor using a two-core fiber (TCF) is proposed and demonstrated. The TCF is designed to operate as a directional coupler with one core located exactly at the center of the fiber and the other off-axis, but close to the center of the fiber. This design allows straightforward splicing of the TCF to single mode fibers (SMF), and alignment of the off-axis core is not strictly required for optimum operation. The sensor is fabricated by simply splicing a 5 cm long section of TCF between two SMF sections, which provides a sinusoidal spectral response. When the fiber is bent, the coupling parameters are modified due to stress-optic and effective length effects, effectively blue-shifting the sinusoidal spectral response of the sensor and allowing for the measurement of curvature. The sensor exhibits linear response and a sensitivity of −137.87 nm/m^{-1} for curvature ranging from 0 to 0.27 m^{-1}, making it suitable to measure small curvatures with high sensitivity.

OCIS codes: (060.2370) Fiber optics sensors; (120.0280) Remote sensing and sensors; (280.4788) Optical sensing and sensors.

References and links

1. M. J. Gander, W. N. MacPherson, R. McBride, J. D. C. Jones, L. Zhang, I. Bennion, P. M. Blanchard, J. G. Burnett, and A. H. Greenaway, "Bend measurement using Bragg gratings in multicore fibre," Electron. Lett. **36**(2), 120–121 (2000).
2. Y. G. Han, X. Dong, J. H. Lee, and S. B. Lee, "Simultaneous measurement of bending and temperature based on a single sampled chirped fiber Bragg grating embedded on a flexible cantilever beam," Opt. Lett. **31**(19), 2839–2841 (2006).
3. Y. Liu, L. Zhang, J. A. R. Williams, and I. Bennion, "Optical bend sensor based on measurement of resonance mode splitting of long-period fiber grating," IEEE Photon. Technol. Lett. **12**(5), 531–533 (2000).
4. C. C. Ye, S. W. James, and R. P. Tatam, "Simultaneous temperature and bend sensing with long-period fiber gratings," Opt. Lett. **25**(14), 1007–1009 (2000).
5. F. Pang, W. Liang, W. Xiang, N. Chen, X. Zeng, Z. Chen, and T. Wang, "Temperature-insensitive bending sensor based on cladding-mode resonance of special optical fiber," IEEE Photon. Technol. Lett. **21**(2), 76–78 (2009).
6. H. Dobb, K. Kalli, and D. J. Webb, "Temperature-insensitive long period grating sensors in photonic crystal fibre," Electron. Lett. **40**(11), 657–658 (2004).
7. T. Allsop, A. Gillooly, V. Mezentsev, T. Earthgrowl-Gould, R. Neal, D. J. Webb, and I. Bennion, "Bending and orientational characteristics of long period gratings written in D-shaped optical fiber," IEEE Trans. Instrum. Meas. **53**(1), 130–135 (2004).
8. O. Frazão, S. F. O. Silva, J. Viegas, J. M. Baptista, J. L. Santos, J. Kobelke, and K. Schuster, "All Fiber Mach–Zehnder Interferometer Based on Suspended Twin-Core Fiber," IEEE Photon. Technol. Lett. **22**(17), 1300–1302 (2010).
9. H. Kogelnik and R. V. Schmidt, "Switched directional couplers with alternating Δβ," IEEE J. Quantum Electron. **12**(7), 396–401 (1976).
10. K. Okamoto, *Fundamentals of Optical Waveguides,* 2nd Ed. (Academic Press - Elsevier, 2006), Chap. 1.
11. A. W. Snyder and P. Richmond, "Effect of anomalous dispersion on visual photoreceptors," J. Opt. Soc. Am. **62**(11), 1278–1283 (1972).
12. Y. Murakami and S. Sudo, "Coupling characteristics measurements between curved waveguides using a two-core fiber coupler," Appl. Opt. **20**(3), 417–422 (1981).
13. E. P. Popov, *Mechanics of Materials,* 2nd Ed. (Prentice Hall, 1976), Chap. 9.
14. S. P. Timoshenko, *Strength of Materials. Part 1,* 2nd Ed. (D. Van Nostrand Company, 1940), Chap. 8.

#186504 - $15.00 USD Received 7 Mar 2013; revised 23 Apr 2013; accepted 27 Apr 2013; published 8 May 2013

15. K. Okamoto, T. Hosaka, and T. Edahiro, "Stress analysis of optical fibers by a finite element method," IEEE J. Quantum Electron. **17**(10), 2123–2129 (1981).
16. A. J. Barlow and D. N. Payne, "The stress-optic effect in optical fibers," IEEE J. Quantum Electron. **19**(5), 834–839 (1983).
17. N. Lagakos, R. Mohr, and O. H. El-Bayoumi, "Stress optic coefficient and stress profile in optical fibers," Appl. Opt. **20**(13), 2309–2313 (1981).
18. P. Rugeland and W. Margulis, "Revisiting twin-core fiber sensors for high-temperature measurements," Appl. Opt. **51**(25), 6227–6232 (2012).

1. Introduction

The measurement of relative displacements and deformations play an important role in different areas such as aerospace, geophysics, nanotechnology, and structural health monitoring. Due to its relation with important structural mechanical parameters such as stress and position, curvature sensing becomes essential to sketch the mechanical conditions of the structures. A growing interest on curvature sensors based on optical fibers has arisen due to their well known superior advantages, such as immunity to external electromagnetic interference, compactness, high sensitivity, and *in situ* measurements. In this regard, a variety of fiber-based curvature sensors can be found in the literature, being the most widely studied those based on fiber gratings and specialty fibers.

Among grating-based curvature sensors, those using fiber Bragg gratings (FBG) as the sensing element can operate in large ranges of curvature (over several m^{-1}) but exhibit low sensitivity (a few hundreds of pm/ m^{-1}). For instance, a FBG in a multi-core (four cores) fiber operating over a curvature range from 0 to 18 m^{-1} with a sensitivity of 48.9 pm/m^{-1} [1] and a sampled chirped FBG embedded in a flexible cantilever structure operating in the range from 0.82 to 2.61 m^{-1} with a sensitivity of 0.56 nm/m^{-1} [2], have been reported. On the other hand, long-period fiber gratings (LPFG) have also been reported and exhibit the highest sensitivity around 14 nm/m^{-1} [3, 4]. The main issue for both LPFG is that they are not capable to measure curvatures less than 0.4 m^{-1}. In the case of specialty fibers, a curvature sensor based on a double-cladd fiber has been reported to operate in the range from 0 to 1.48 m^{-1} with a sensitivity of 10.15 nm/m^{-1} [5]. Furthermore, several alternatives for curvature sensing on which the grating is inscribed in the specialty fibers have been also reported. For instance, an arc-induced LPFG on a photonic crystal fiber (PCF) has been reported to operate in the range from 0 to 1 m^{-1} with a sensitivity of 3.70 nm/m^{-1} [6], while an ion-laser-induced LPFG on a D-shaped fiber has been reported to operate in the curvature range from 0.5 to 4 m^{-1} with sensitivity of 12.55 nm/m^{-1} [7]. The main issues in FBG based curvature sensors, regardless of the kind of fiber where they are inscribed, are related to the need to inscribe the grating which involves not only expensive equipment, but also to the low sensitivities that can be achieved. More recently interferometric alternatives have been also reported. Despite the fact that interferometric sensors exhibit high sensitivities, this is not the case for curvature sensors. An in-fiber Mach-Zehnder interferometer for curvature sensing has been reported to operate in the range from 0.1 to 1.7 m^{-1} with a sensitivity of −2.56 nm/m^{-1} [8]. Although this sensor is simple to fabricate, a relatively long fiber is needed to induce significant changes in the interferometric pattern. The common feature in the reported sensors is that they are not capable of measuring small curvatures due to their low sensitivity.

In this paper a simple, compact, and cost-effective fiber optic curvature sensor based on a two-core fiber (TCF) is demonstrated. The TCF is designed to operate as a directional coupler with one core located exactly at the center of the fiber and the other off-axis, but close to the center of the fiber. This design allows regular splicing procedures of the TCF to SMF, and eliminates any alignment of the off-axis core with respect to the bending plane. When the fiber is bent, the coupling parameters are modified due to stress-optic and effective length effects, which effectively blue-shifts the spectral response of the sensor and allow us to measure the curvature. The sensor exhibits linear response in the range from 0 to 0.2653 m^{-1}, with a sensitivity of −137.8763 nm/m^{-1}, which is at least nine times better as compared to the most sensitive sensors reported to date [3, 4].

#186504 - $15.00 USD Received 7 Mar 2013; revised 23 Apr 2013; accepted 27 Apr 2013; published 8 May 2013

2. Principle of operation

The cross section of the TCF used as the sensing element of the curvature sensor is shown in Fig. 1(a). The diameter of the cladding is the standard 125µm and it has two cores, both with a diameter of 8.6 µm. One of the cores is located exactly at the center of the fiber axis, while the other is asymmetrically located with a distance of 15 µm between the centers of the cores. The refractive index of the core and cladding are 1.448 and 1.443 respectively, with a numerical aperture of NA = 0.12. The fiber was manufactured at ACREO Fiberlab, in Sweden. According to the manufacturers, the fabrication of the fiber was achieved by drilling a hole in the preform of a standard telecom fiber and then inserting the second core. The fiber was designed to accomplish two key functions. Firstly, the separation of the cores is small enough to allow overlapping between the modes of the cores, such that the fiber operates as an optical directional coupler. Additionally, since one of the cores of the TCF is located at the center of the fiber, splicing it to a SMF is straightforward, without the need of special or complex procedures.

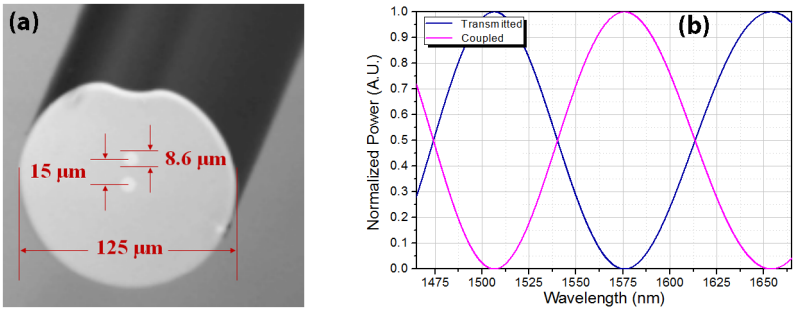

Fig. 1. (a) Cross-section of the Two-Core Fiber. (b) Spectral response of the TCF in the spectral window from 1465 nm to 1665 nm.

Given the characteristics of the TCF, the sensor is easily fabricated by just splicing a 50 mm long section of TCF between two SMF. The natural arising implication is that only the central core will be excited at the input of the TCF, allowing us to treat the central core as the transmitting waveguide while the external core is treated as the coupling waveguide. Under this condition and if the fiber is held straight (zero stress), the propagation constant of the fundamental mode of both waveguides is the same. The transmitted power is then defined as a cosine square function of the coupling constant. Therefore, when a broadband source with constant power is coupled to the sensor, the power will be coupled back and forth between the center and outer cores as shown in Fig. 1(b). Since the input and output SMF are coupled to the center core of the TCF, from now on we will only focus on the response of the transmitting waveguide. According to the mathematical formulation for modeling the mutual light-wave interactions between two parallel optical fibers, the coupling coefficient κ can be calculated from the following expression [9–12],

$$\kappa = \frac{\sqrt{2\Delta}}{a} \cdot \frac{U^2 K_0\left(\frac{W \cdot s}{a}\right)}{V^3 \left[K_1(W)\right]^2} \tag{1}$$

where a is the radius of the cores of the TCF, s is the center to center separation distance between them, and Δ is the relative refractive index difference. K_0 and K_1 are the modified Hankel functions of order 0 and 1, respectively; V is the normalized frequency (i.e. V parameter), and U and W are the normalized transverse propagation constants of the LP_{01} mode in the core and cladding, respectively [10]. Based on Eq. (1) we can notice that the coupling process is sensitive to both optical and geometrical conditions [12]. Therefore any change in the structure of the TCF, either optical or geometrical, will modify the coupling

#186504 - $15.00 USD Received 7 Mar 2013; revised 23 Apr 2013; accepted 27 Apr 2013; published 8 May 2013

coefficient and then the response of the TCF. It is worth to point out that the parameters Δ, U, V, W, K_0, and K_1 appearing in Eq. (1) are dependent on the actual refractive indices of both core and cladding as they are actually defined in terms of these refractive indices [10,12].

When the TCF is bent there are two main effects simultaneously acting on the fiber that can modify its spectral response: the stress-optic effect and the effective-length effect. The stress-optic effect is related to changes in the refractive index of certain material due to mechanical stress. Therefore, when the fiber is bent there will be some stress acting on the fiber that will induce slight changes on the refractive index of both core and cladding thus modifying all the variables previously mentioned and then affecting directly the coupling coefficient, as can be noticed from Eq. (1).

In our particular case the fiber is assumed to be bonded to two translation stages, one remains fixed and one movable, and the polymeric coating is to be removed from the fiber in the bending section. If the fiber is carefully aligned, bending will occur only along the plane defined by the axis of the movable stage and the displacement of the fiber. In other words, twisting of the fiber can be avoided by accurate alignment. Therefore, since twisting of the TCF is negligible and only bending is considered, the column theory can be suitable instead of the flexible tube model, in order to model the behavior of the TCF [13,14]. Based on the column theory, the stress induced to the fiber can be calculated in terms of the axial load which, in turn, is defined in terms of the vertical deflection, the geometrical parameters of the fiber, and the material properties, as shown in Eq. (2). In Eq. (2), the stress on the fiber can be calculated directly from the axial load $\boldsymbol{P}$ acting on the cross sectional area of the fiber $\boldsymbol{A}$; $\boldsymbol{E}$ is the Young's modulus, $\boldsymbol{I_z}$ is the moment of inertia, $\boldsymbol{d}$ is the vertical deflection with respect to the horizontal, $\boldsymbol{L}$ is the length of the fiber between the bases, and $\boldsymbol{e}$ is the so-called eccentricity, which refers to a geometrical condition that indicates how much the axial load is shifted with respect to the center of the cross sectional area. Based in our previous bending scenario, $\boldsymbol{e}$ can be assumed to be $\boldsymbol{e} = (2\text{x}10^{-4})\boldsymbol{d}$. This relation between the eccentricity and the vertical deflection, which finally results in a very small value of eccentricity, represents the practical condition in which the fiber is aligned and the axial load acts approximately in the center of the cross section of the fiber.

$$\sigma = \frac{P}{A} = \frac{\left({2EI_z d}/{eL^2} \right)}{A} \tag{2}$$

Once the stress acting on the fiber has been calculated, it can be directly transformed into a refractive index change for both core and cladding assuming a constant stress-optic coefficient of $\boldsymbol{C_{str\text{-}opt}} = -\ 3.3\text{x}10^{-6}$ mm^2/N, by using the following expression [15–17]:

$$\Delta n = C_{str-opt}\sigma \tag{3}$$

After the refractive index change corresponding to a specific curvature is calculated, using Eq. (2) and then Eq. (3), then the coupling coefficient for this new condition can be computed by recalculating the variables appearing in Eq. (1) by taking into account the corresponding refractive index change. Figure 2 shows the spectral behavior of the coupling coefficient between the cores for several curvature conditions. It can be clearly noticed that the tendency of the spectral response of the coupling coefficient is preserved but it shifts as the curvature increases, which is expected due the change induced on the refractive indices via stress.

#186504 - $15.00 USD Received 7 Mar 2013; revised 23 Apr 2013; accepted 27 Apr 2013; published 8 May 2013

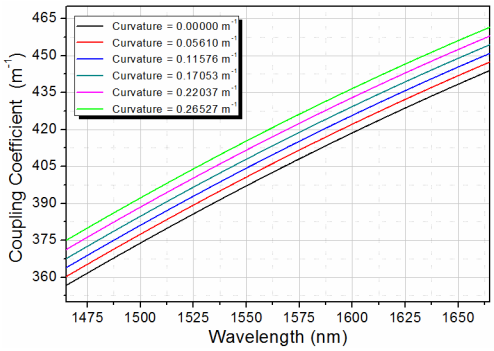

Fig. 2. Spectral behavior of the coupling coefficient.

Based on the coupling theory for a directional coupler, the spectral response of the normalized power in the central core, for the case in which only the central core is excited at z = 0, can be calculated using Eq. (4) [10–12],

$$P_{Trans}(z) = \cos^2\left(\sqrt{\kappa^2+\delta^2}\, z\right) + \frac{\delta^2}{\kappa^2+\delta^2}\sin^2\left(\sqrt{\kappa^2+\delta^2}\, z\right) \tag{4}$$

where z corresponds to the propagation distance and δ is a parameter related to the difference between the propagation constants of core and cladding. Since both cores have the same optical properties, we can assume that both cores have the same propagation constant and thus δ to be equal to zero. Based on this assumption, and the fact that the TCF will have a finite length L_0, the transmitted power as a function of wavelength is then obtained by Eq. (5) using the coupling constant values obtained in Fig. (2).

$$P_{Trans}(\lambda, C) = \cos^2\left[\kappa(\lambda, C) L_0\right] \tag{5}$$

Regarding the effective length effect, according to the column theory developed in mechanics of materials, the effective-length effect arises when the fiber is bent since an equivalent configuration of the system can be depicted when the translation stage is slightly displaced forward [13,14]. The effect of the effective length will manifest in the generation of an equivalent configuration where the length of the TCF is either increased or decreased, depending on the direction of the displacement of the stage, and effectively shifts the TCF fiber transmitted spectrum.

In order to observe the individual impact of both effects, the curvature sensor response was simulated independently for stress and effective length. The spectral response of the TCF curvature sensor was simulated assuming constant stress-optic coefficient and constant TCF length for the case of the stress-optic effect, while constant decreasing rate of the length of the TCF section was assumed for the case of the effective-length effect. A total wavelength blue-shift of about 39 nm is obtained for the curvature range from 0 m^{-1} to 0.2653 m^{-1}, as shown in Fig. 3(a), with an approximate linear relationship between the curvature and the effective refractive index with a slope of ~830 nm/Refractive Index Unit (RIU). This means that, in terms of curvature sensing, a sensitivity of –147 nm/m^{-1} can be achieved by only considering the stress-optic effect, as shown in Fig. 3(c). On the other hand, the effective-length effect was studied by applying horizontal displacements in the range from 0 μm to 250 μm, which corresponds to the same curvature range from 0 m^{-1} to 0.2653 m^{-1} mentioned above. A total wavelength red-shift of about 2 nm is obtained, as shown in Fig. 3(b), with a good linear relationship between the curvature and the horizontal displacement with a slope of ~8,000 nm/m. This provides a sensitivity of 7.5 nm/m^{-1}, as shown in Fig. 3(c), for curvature sensing when only the effective-length effect is taken into account. When the combined effect is considered and both contributions are taken into account, a sensitivity of approximately –137 nm/m^{-1} can be achieved for curvature measurements in the range from 0 m^{-1} to 0.2653 m^{-1}, as

#186504 - $15.00 USD Received 7 Mar 2013; revised 23 Apr 2013; accepted 27 Apr 2013; published 8 May 2013

shown in Fig. 3(c). The net result is a total wavelength blue-shift of about 37 nm is obtained for this curvature range. Therefore, in the small-curvature regime refractive indices changes due to stress-optic effects are the dominating terms, while small changes are produced due to effective changes of the TCF length.

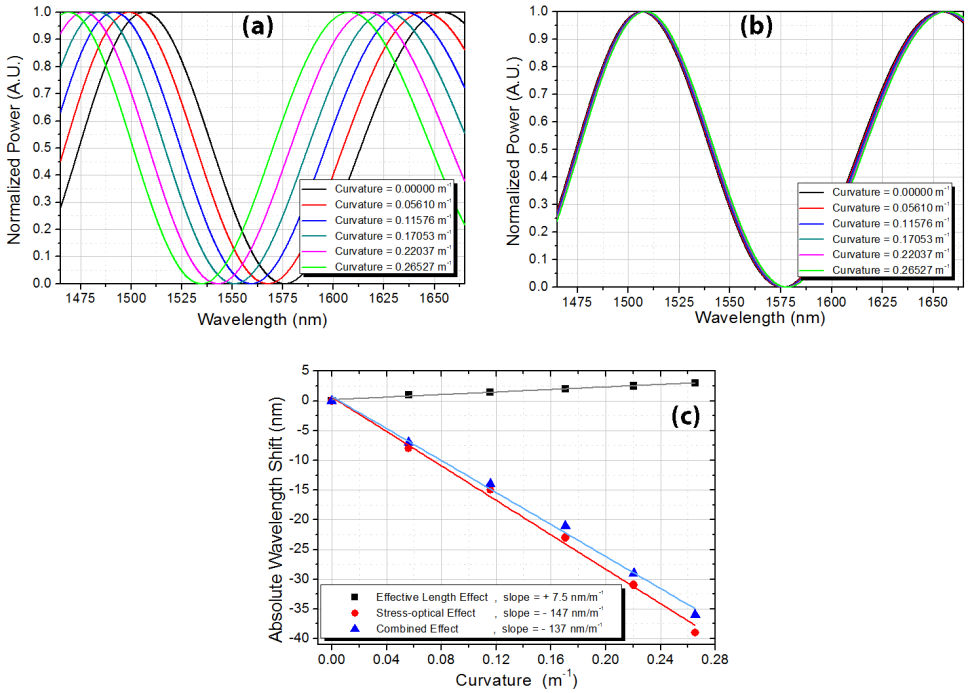

Fig. 3. Spectral response of the TCF due to (a) stress-optic effect, (b) changes in the effective length, and (c) absolute wavelength shift as a function of the applied curvature.

The simulations shown in Fig. 3 correspond to off-axis core aligned with the bending plane. However, when a fiber is bent, the inner part of the fiber (smallest radius of curvature) is subjected to compressive strain, while the outer part of the fiber (largest radius of curvature) is subjected to tensile strain. This means that cores located at opposite positions, with respect to the fiber axis and parallel to the bending plane of the fiber, will experience similar stress-optic effects but with different signs. It also means that if an off-axis core is parallel or perpendicular to the bending plane, we should also have different stress-optic effects. The net result in our TCF is that the position of the off-axis core should exhibit a different stress-optic effect as compared to that of the on-axis core. However, in our TCF the separation of the cores is small enough for such effect to become considerable, and we can neglect effects related to the orientation of the off-axis core from our simulations regarding stress-optic effects. This was experimentally corroborated as it will be later described. Therefore, in our simulations the stress-optic effects will change the refractive index of both core and cladding of the TCF due to the induced curvature, but having the same sign.

3. Experiment and results

The curvature sensor is fabricated by splicing a 50 mm section of TCF between two SMF. In order to control the alignment of the cores with respect to the bending plane, the TCF fiber is first spliced to a SMF and then the TCF is cleaved to have a length of 50 mm. After this the SMF-TCF segment is inserted in a copper tube holder and using a CCD camera the axis of the cores is identified and labeled in the copper tube. The cleaved end of the TCF is finally spliced to the second SMF and the curvature sensor is fabricated. This allows a simple way to align the cores either parallel or perpendicular to the bending plane.

#186504 - $15.00 USD Received 7 Mar 2013; revised 23 Apr 2013; accepted 27 Apr 2013; published 8 May 2013

A schematic of the experimental setup for testing the curvature sensor is shown in Fig. 4. The input SMF is connected to a polarization controller (PC), and the PC is connected to a super luminescent diode (SLD) which acts as a broadband light source centered at 1580 nm. The output SMF is sent to an optical spectrum analyzer (OSA) to monitor the spectrum of the transmitted signal. A segment of fiber, with the TCF section at the center, is held between two translation stages. One of the stages is fixed while the other one is able to move in order to allow bending of the TCF when it moves closer to the other stage. The separation between the bases equals 2L, where L is the length of the TCF (i.e. the separation between the bases is 100 mm). Under this scenario the radius of curvature can be easily estimated using the equation shown in Fig. 4 [8].

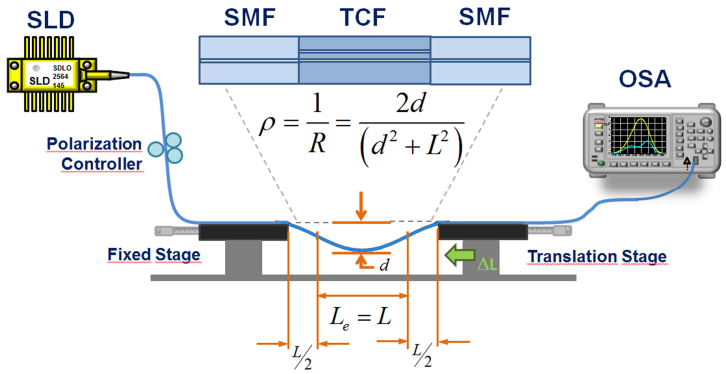

Fig. 4. Experimental characterization setup of the TCF curvature sensor.

Before performing the characterization of the sensor, its response under different polarizations and alignments of the off-axis core with respect to the bending plane was investigated. The polarization is carefully changed using the PC in steps of 45° and the response is monitored using the OSA. We observed that the spectral response is not significantly affected since the spectrum is not shifted when the polarization is modified, and there is only a minor change of the transmitted intensity which is less than 1%. Therefore, the polarization was fixed parallel to the bending plane to keep consistency in our measurements. In order to observe the response as a function of the alignment of the off-axis core, the response of the sensor was acquired for three different curvatures at three different off-axis core positions: 0°, 45°, and 90° with respect to the bending plane. We can notice a slight difference of less than 0.5 nm in the blue-shift when the core is perpendicular and aligned to the bending plane. We believe that this is probably due to a small difference between the stress-optic effects induced in the cores. Nevertheless, the difference is very small to induce a significant error as compared to our simulations. Based on these results, during the characterization of the sensor the polarization of the SLD and the off-axis core are aligned to the bending plane. The sensor was tested by moving the translation stage in steps of 50 μm, and the transmitted spectrum is acquired at each step with the OSA. At each step the variable ***d*** is also measured and the curvature value is estimated from the equation shown in Fig. 4.

The experimental results of the curvature sensor based on the TCF are shown in Fig. 5(a), where the transmitted spectrum is plotted for different values of curvature (i.e. inverse of radius of curvature). As expected, the full waveform of the spectral response experience a blue-shift as the fiber bends. We can observe that the shifting is quite uniform, and that the waveform is not deteriorated as the fiber bends. There are only small variations in the peak intensity during bending which we believe are due to slight misalignment of the fiber with respect to the bending plane. Figure 5(b) shows the absolute wavelength shift of the sensor. A total wavelength shift of −36.93 nm was achieved for the curvature range from 0 to 0.2653 m^{-1}. As shown in the inset of Fig. 5(b), a linear response with a slope of −137.87 nm/m^{-1} and R^2 higher than 0.9973 is achieved. Experimental results differ from numerical simulations in less than 1%, which confirms the accuracy of the theoretical modeling. It is important to

#186504 - $15.00 USD Received 7 Mar 2013; revised 23 Apr 2013; accepted 27 Apr 2013; published 8 May 2013

highlight that the sensor is capable of measuring larger values of inverse radius of curvature by using a shorter section of TCF in order to achieve a larger free spectral range (FSR). However, due to our narrow spectral window it was not feasible to follow the blue shift of the same peak beyond the reported curvature range.

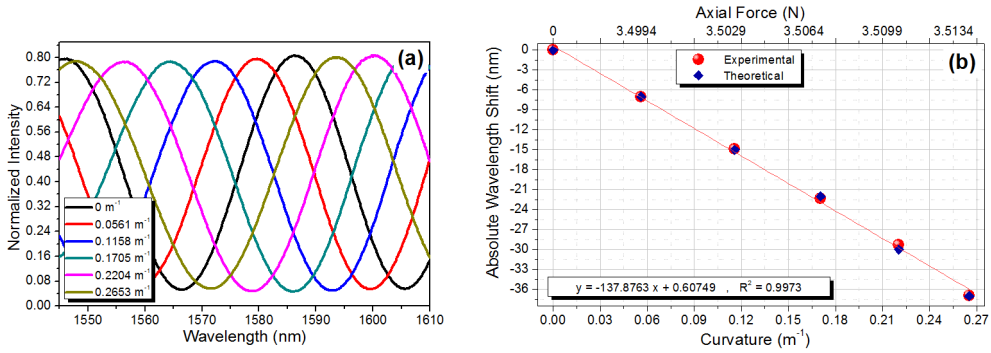

Fig. 5. (a) Spectral response of the TCF-based curvature Sensor. (b) Absolute wavelength shift with respect to curvatures: comparison between experimental and theoretical results.

We can also estimate the stress profile of the fiber based on the column theory. By considering the proposed scheme as a beam with built-in ends submitted to compressive axial loads (the fiber is fixed to both stages), the acting forces can be easily estimated [13,14]. As shown in Fig. 5(b), we can correlate the sensor blue-shift to the axial forces acting on the fiber. This is particularly important because, given the high sensitivity of the sensor, the sensor can be embedded in a structure and could be potentially used to measure the axial strain applied to the structure. We should also mention that the sensitivity of the sensor can be easily increased by decreasing the separation between the cores. As shown in Fig. 6(a), as the center to center core separation is reduced the sensitivity is significantly increased. Such modification can be done by either drawing a new fiber or tapering a section of the fiber to reduce the total diameter of the actual TCF.

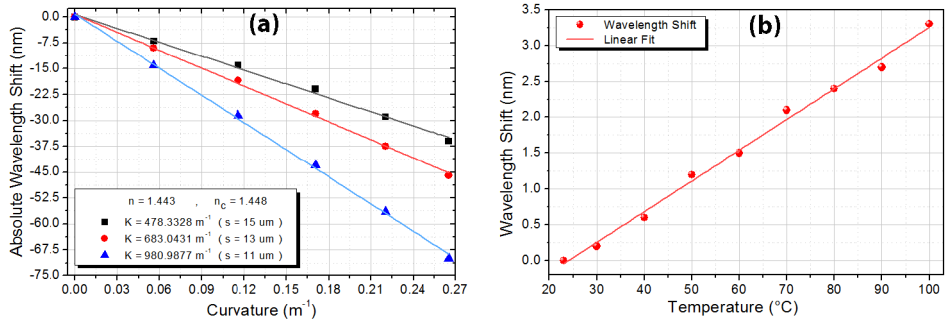

Fig. 6. (a) Absolute wavelength shift of the sensor as a function of the applied curvature for different separations between the cores. (b) Temperature response of the curvature sensor.

Since the sensor operates based on the spectral shift of the TCF response, temperature effects need to be taken into account. The temperature dependence of the curvature sensor was disclosed by measuring the spectral shift for the temperature range from 23 °C to 100 °C. In order to perform measurements where only the temperature effect is to be considered, the fiber was kept straight in all times and the polarization was set to be unaltered by using a polarization controller. Additionally, since the sensor response was measured for temperatures not larger than 100 °C, no thermal pre-treatment was applied to the fiber. Figure 6(b) shows the spectral shift of the TCF response with respect to the response at 23 °C. A total red shift of approximately 3.3 nm was obtained at 100 °C. The linear fit of the experimental measurements suggest a monotonic temperature dependence of 42.88 ± 1.18 pm/°C, which is

#186504 - $15.00 USD Received 7 Mar 2013; revised 23 Apr 2013; accepted 27 Apr 2013; published 8 May 2013

similar to that reported for a high-temperature sensor using this same TCF [18]. Although the temperature sensitivity is not very high, in order to obtain accurate curvature measurements temperature effects has to be taken into account.

4. Conclusion

In summary, a novel, simple, and cost-effective curvature sensor based on a TCF has been demonstrated. The key advantages of the sensor are related to the simple splicing of the TCF and SMF, alignment of the off-axis core is not strictly required for optimum operation, and the sensitivity is significantly enhanced as compared to other fiber based curvature sensors. The mean error between the theoretical analysis and experimental data was less than 1%, which confirms the reliability of the theoretical model. The sensor exhibits linear response in the range from 0 to 0.2653 m^{-1}, with a sensitivity of −137.8763 nm/m^{-1}. Compared to grating-based and specialty fibers curvature sensors reported in the literature, the sensor exhibits a sensitivity 9.8 and 10.9 times higher, respectively. While most of the grating-based curvature sensors reported in literature are not capable of measuring small curvatures, the demonstrated sensor exhibits very high sensitivity in making such measurements, making it suitable for high-performance curvature measurements.

Acknowledgment

We sincerely appreciate the support from the Consejo Nacional de Ciencia y Tecnología (CONACyT) under contract CB-2010/157866. J. R. Guzman-Sepulveda acknowledges CONACyT for their support through a M.Sc. scholarship. We are also very grateful to Dr. Walter Margulis for useful discussions and comments. The TCF used in this work was fabricated at Acreo's Fiberlab.

#186504 - $15.00 USD Received 7 Mar 2013; revised 23 Apr 2013; accepted 27 Apr 2013; published 8 May 2013